

A statistical mechanical analysis on the possibility of achieving fair cylindrical dice

M. N. C. Brustelo,* M. M. Vivaldi,[†] and F. Marques[‡]

*University of São Paulo, Institute of Physics,
66318, 05315-970, São Paulo, SP, Brazil*

(Dated: November 30, 2023)

Many have dedicated their time trying to determine the ideal conditions for a cylinder to have equal probabilities of falling with one of its faces facing upwards or on its side. However, to this day, there is no concrete analysis of what these conditions should be. In order to determine such circumstances, a theoretical analysis was conducted, considering approaches from Rigid Body Dynamics and Statistical Mechanics. An experimental system was also built to improve control over the launches, and a comparative analysis was performed between the results obtained experimentally and the theory. It was concluded that the environment and other launching conditions have a significant influence; nevertheless, it is possible, under controlled conditions, to determine, within certain limits, the expected probabilities.

arXiv:2311.17079v1 [physics.class-ph] 27 Nov 2023

*E-mail: matheus.brustelo@gmail.com

[†]E-mail: mateusmvivaldi@gmail.com

[‡]E-mail: fabriciomarques@if.usp.br

I. INTRODUCTION

When studying probability and statistics, it is common to encounter examples of a cubic die or of coins that can be flipped to heads or tails. Although one can consider cases of a biased die, where most of the mass is concentrated near the face opposite to the one that is more likely to end up facing upwards, there is no *a priori* reason to expect that each face of the cube does not have an equal probability of $1/6$ of ending up facing upwards. Similarly, in the case of a coin, if a large number of tosses are performed, the common expectation is to obtain heads for approximately half the number of tosses and tails for the remaining half. However, in the case of the coin, we can observe an interesting fact. Most coins are cylinders that have a small thickness H compared to their radius R . It is possible, with some care and patience, to balance a coin with its side resting on a horizontal flat surface, so that it is neither in the “heads” nor “tails” state, but rather in a third state, which we can call the “side” state. Much less likely, obviously, is for the coin to end up in this position after an arbitrary toss.

Just as the idea of a coin landing in the “side” state after a toss seems extremely improbable, it may also appear nonsensical to expect that a stick, which is nothing more than a cylinder with $H \gg R$, ends up in a state equivalent to “heads” or “tails”, i.e., with one of its faces facing downwards, after being thrown. Unlike the case of the coin, therefore, the common expectation is for the stick to end up in the “side” state when landing on a flat and horizontal surface.

The combination of the common expectations for the coin and the stick, therefore, leads us to the question proposed in the statement of Problem 7 of the 35th International Young Physicists’ Tournament 2022 (IYPT 2022) [1, 2] :

“To land a coin on its side is often associated with the idea of a rare occurrence. What should be the physical and geometrical characteristics of a cylindrical dice so that it has the same probability to land on its side and one of its faces?”

In other words, for a cylinder, the probability of obtaining “face” is $P_F \approx 1$, and the probability of obtaining “side” is $P_S \approx 0$ for $H \ll R$ (coin). On the other hand, these same probabilities become $P_F \approx 0$ and $P_S \approx 1$ for $H \gg R$ (stick). However, there could be some ideal H/R ratio that, combined with a certain set of specific physical conditions, would make

$P_S = 1/3$ and $P_F = 2P_{F_1} = 2P_{F_2} = 2/3$. If the right set of conditions could be determined, we would then have a “fair cylindrical die”.

Besides the specific problem proposed in IYPT 2022, which requires the analysis of a cylindrical die, the idea could, in principle, be generalized to analyze the conditions that allow the construction of fair dice with different geometries. In role-playing games, for example, it is common to use dice with shapes different from the typical cubic form. An interesting mathematical analysis concerning the allowed forms for convex polyhedra to be considered suitable candidates to constitute “fair dice” can be found in reference [3]. That study, though, does not take into account the physics of a launch, but instead will focus on symmetry group arguments. A comment is made about other fair polyhedra, including a solid produced by cutting off the tips of a di-pyramid with $2n$ identical triangular faces with two planes parallel to its base and equidistant from it. Following that comment, they point out that the location of those cuts would possibly depend on mechanical properties of such a die and also of the surface where it will land. To justify that statement, they cite an early paper [4] that proposes to analyze the motion of a tossed coin in order to seek for its connections with the probabilities of getting heads or tails, but restricted to the situation of vertical launches with landings on a plane surface which completely absorbs the impact, as sand or mud. In this context, our cylinders can be considered an extended version of the cutted di-pyramids described by [3] in a limit in which n and the height of the di-pyramid are taken to be infinite, but the two cuts are made at a finite distance from each other, which will be the height H of the cylinder. Also, instead of restricting ourselves to a complex yet restrictive study on the mechanics of a cylinder’s motion, we will move towards a statistical mechanical analysis, therefore presenting a different perspective about this matter.

This work is organized as follows. Section II will present some of the technical aspects of the statistical interpretation of results from cylindrical dice rolls, as well as the theory associated with the motion of a cylindrical rigid body. In Section III, a general description of the experimental apparatus used will be provided. Next, in Section IV, the obtained data will be presented along with their respective analysis and discussion. Finally, in Section V, the concluding remarks will be presented.

II. THEORETICAL FOUNDATIONS

A. Free motion of a cylinder falling under the action of gravity

The position \vec{R} of the Center of Mass (CM) of a rigid body with respect to an inertial reference frame is affected by external forces acting on the body. In the case of the cylindrical die, during its flight motion, the weight force and air resistance forces come into play. For sufficiently small cylinders, launched at low heights to avoid reaching high velocities, air resistance forces can be neglected as a first approximation. These forces, in addition to affecting the CM position, could also influence the angular velocity of the cylinder, particularly around an axis contained in the plane defined by the principal axes x_1 and x_2 .

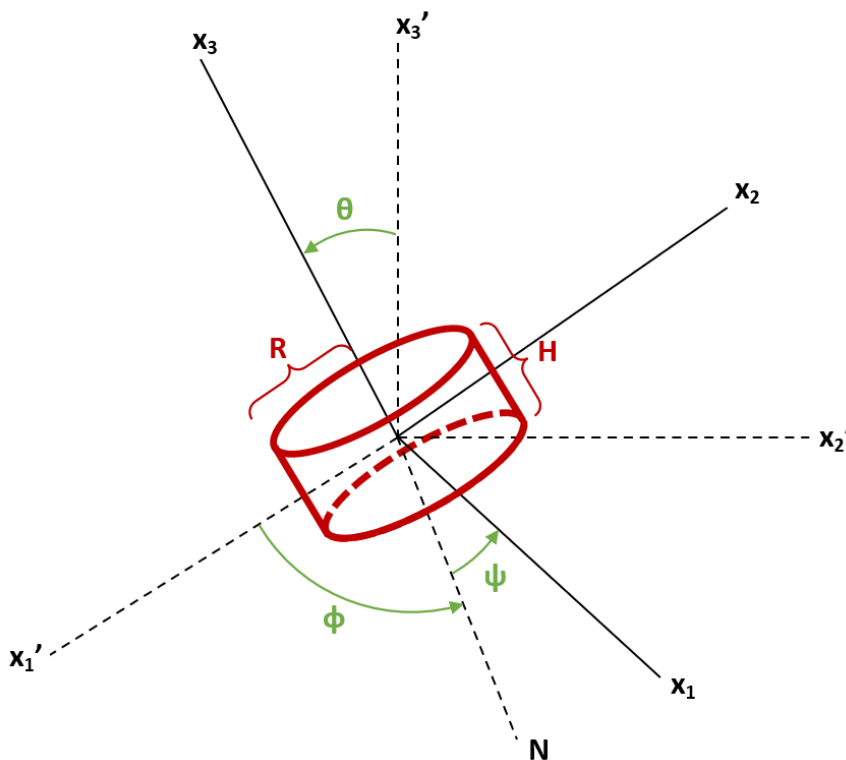


FIG. 1: Fixed orientation system S' , body's principal system S , and the Euler angle convention to be used.

In this regard, a theory that does not consider the air resistance forces is limited in not taking into account the aerodynamics of the cylinder's motion, which can make the initial collision of “face” or “side” more or less probable. However, unless a set of materials is chosen

for the cylinder and surface such that the cylinder sticks to the surface upon collision, the final state will only occur after a sequence of multiple collisions. On the other hand, the weight force acts as if it were concentrated entirely on the CM, not affecting the rotational motion of the cylinder during its flight.

Therefore, in the approximation that neglects the dissipative forces exerted by the contact with air, we can analyze the flight motion of the cylindrical die as the free rotational motion of a rigid body whose CM translates by inertia in the horizontal direction and under the influence of weight in the vertical direction. In this motion, mechanical energy E and angular momentum l are conserved quantities. The rotational motion is governed by how mass is distributed within the cylinder. For a homogeneous mass distribution in a cylinder with radius R , height H , and mass M , the principal moments of inertia will be:

$$I_1 = I_2 = I = \frac{MR^2}{4} + \frac{MH^2}{12} \quad \text{and} \quad I_3 = \frac{MR^2}{2} \quad (1)$$

and the mechanical energy can be written as:

$$E = \frac{MV^2}{2} + \frac{I_1\omega_1^2}{2} + \frac{I_2\omega_2^2}{2} + \frac{I_3\omega_3^2}{2} + Mgh \quad (2)$$

where $V = |\dot{\vec{R}}|$ is the velocity of the CM, h is the height of the CM relative to the level of the horizontal plane where the cylinder will land, and ω_1 , ω_2 , and ω_3 are the components of the angular velocity vector of the cylinder in the principal axis system.

The terms in Equation (2) proportional to the moments of inertia correspond to rotational kinetic energy. Using Euler angles as defined in Figure 1, the components of the angular velocity can be written as:

$$\omega_1 = \dot{\phi} \sin \theta \sin \psi + \dot{\theta} \cos \psi, \quad \omega_2 = \dot{\phi} \sin \theta \cos \psi - \dot{\theta} \sin \psi \quad \text{and} \quad \omega_3 = \dot{\phi} \cos \theta + \dot{\psi} \quad (3)$$

Substituting the expressions (3) for the components of the angular velocity in (2), considering the symmetry of the mass distribution that makes $I_1 = I_2 = I$, and assuming a moment immediately before the collision of the cylinder with the landing plane, which makes $h = R \left(\sin \theta + \frac{H}{2R} \cos \theta \right)$, the mechanical energy will be given by:

$$E = \frac{MV^2}{2} + \frac{I}{2} \left(\dot{\phi}^2 \sin^2 \theta + \dot{\theta}^2 \right) + \frac{I_3}{2} \left(\dot{\phi} \cos \theta + \dot{\psi} \right)^2 + MgR \left(\sin \theta + \frac{H}{2R} \cos \theta \right) \quad (4)$$

The angular momentum, by its turn, will have components in the principal system, given by:

$$l_1 = I\omega_1, \quad l_2 = I\omega_2 \quad \text{and} \quad l_3 = I_3\omega_3$$

and, using the expressions (3), we can write the squared magnitude of the total angular momentum, l^2 , which is another constant of the flight motion:

$$l^2 = l_1^2 + l_2^2 + l_3^2 = I^2 \left(\dot{\phi}^2 \sin^2 \theta + \dot{\theta}^2 \right) + I_3^2 \left(\dot{\phi} \cos \theta + \dot{\psi} \right)^2 \quad (5)$$

Changing the sign of the potential energy term in expression (4), we obtain the Lagrangian L , which is cyclic in ϕ and ψ , i.e., it does not depend explicitly on these angles. Therefore, in addition to the mechanical energy E , the canonically conjugate momenta p_ϕ and p_ψ are also constants of motion [5], given by:

$$\begin{aligned} p_\phi &= \frac{\partial L}{\partial \dot{\phi}} = (I \sin^2 \theta + I_3 \cos^2 \theta) \dot{\phi} + I_3 \dot{\psi} \cos \theta \\ p_\psi &= \frac{\partial L}{\partial \dot{\psi}} = I_3 \left(\dot{\phi} \cos \theta + \dot{\psi} \right) = I_3 \omega_3 \end{aligned} \quad (6)$$

and thus, we can rewrite the expression (4) for the mechanical energy as:

$$E = \frac{MV^2}{2} + \frac{I\dot{\theta}^2}{2} + \frac{(p_\phi - p_\psi \cos \theta)^2}{2I \sin^2 \theta} + \frac{p_\psi^2}{2I_3} + MgR \left(\sin \theta + \frac{H}{2R} \cos \theta \right) \quad (7)$$

B. Dynamics of the collision between a cylinder and a horizontal flat surface

The position of the contact point at the instant of collision can be written as:

$$\vec{r} = \rho(\theta)\hat{\rho} - h(\theta)\hat{e}'_3 \quad (8)$$

where $\rho(\theta) = R \left(-\cos \theta + \frac{H}{2R} \sin \theta \right)$, $h(\theta) = R \left(\sin \theta + \frac{H}{2R} \cos \theta \right)$ and $\hat{\rho} = (-\hat{e}'_1 \sin \phi + \hat{e}'_2 \cos \phi)$ is a horizontal unit vector perpendicular to the nodal line $\hat{n} = (\hat{e}'_1 \cos \phi + \hat{e}'_2 \sin \phi)$. The unit vectors $\hat{\rho}$, \hat{n} , and \hat{e}'_3 define an orthonormal basis in space, such that $\hat{\rho} \times \hat{n} = \hat{e}'_3$, $\hat{n} \times \hat{e}'_3 = \hat{\rho}$, and $\hat{e}'_3 \times \hat{\rho} = \hat{n}$ (Fig. 2(a)).

During the contact, the cylinder experiences a normal force $\vec{F} = F\hat{e}'_3$ and a frictional force $\vec{f} = f_\rho\hat{\rho} + f_n\hat{n}$. Therefore, the torque with respect to the center of mass is:

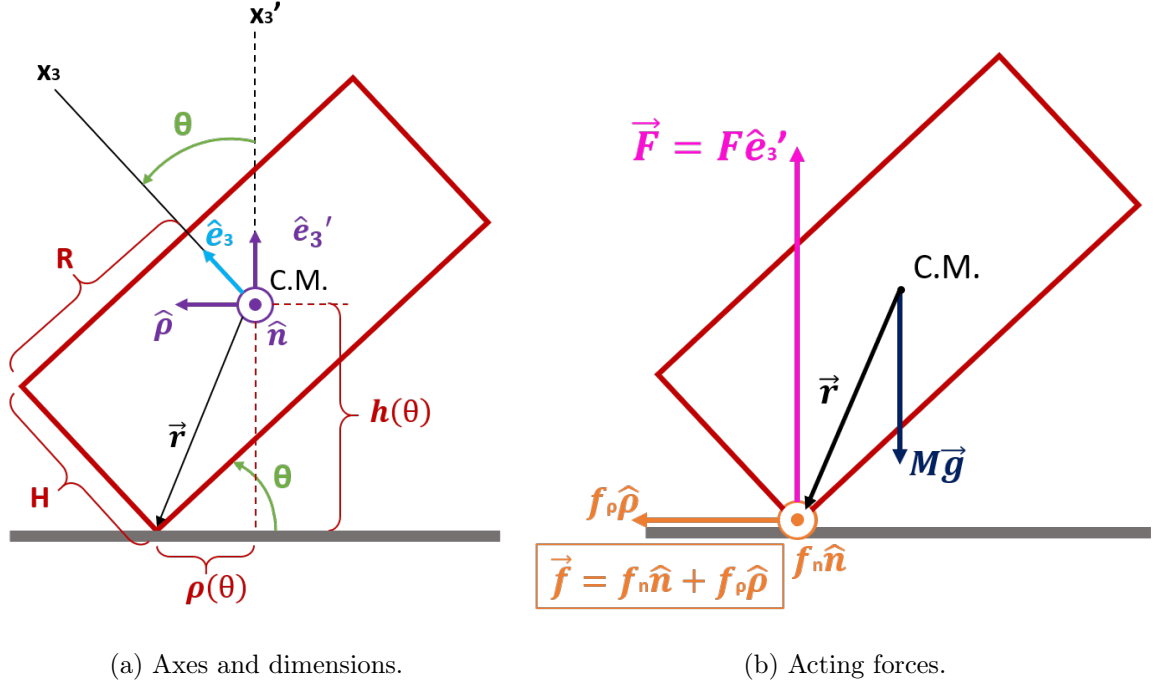


FIG. 2: Geometry of the cylinder system at the instant of collision with the landing plane.

$$\vec{\tau}' = \vec{r} \times (\vec{F} + \vec{f}) = -\left(h(\theta)f_\rho + \rho(\theta)F\right)\hat{n} + f_n\left(h(\theta)\hat{\rho} + \rho(\theta)\hat{e}'_3\right) \quad (9)$$

The torque from the normal force can contribute to changes in the angular frequency $\dot{\theta}$ and the velocity of the center of mass. The frictional torque can have two contributions, one tangential (in the direction of \hat{n}) and one radial (in the direction of $\hat{\rho}$) with respect to the arc that the contact point tends to describe around the vertical axis x'_3 , thus potentially causing changes in all three angular frequencies $\dot{\phi}$, $\dot{\theta}$, and $\dot{\psi}$ (Fig. 2(b)).

The energy W_1 dissipated during the first collision of a given cylinder with the landing plane can receive a contribution W_F due to the normal force \vec{F} , since the collision is not perfectly elastic, and another contribution W_f due to the friction \vec{f} , provided that the cylinder slides on the plane. Therefore:

$$\begin{aligned}
W_1 &= W_F + W_f = \int \vec{F} \cdot d\vec{r} + \int \vec{f} \cdot d\vec{r} \\
&= \int_0^{\Delta t_1} (\vec{F} + \vec{f}) \cdot \vec{v} dt = \int_0^{\Delta t_1} (\vec{F} + \vec{f}) \cdot (\vec{V} + \vec{\omega}' \times \vec{r}) dt \\
&= \int_0^{\Delta t_1} \underbrace{(\vec{F} + \vec{f}) \cdot \vec{V}}_{\vec{F}_{\text{contact}}} dt + \int_0^{\Delta t_1} \underbrace{(\vec{F} + \vec{f}) \cdot (\vec{\omega}' \times \vec{r})}_{\vec{\omega}' \cdot (\vec{r} \times \vec{F}_{\text{contact}}) = \vec{\omega}' \cdot \vec{\tau}'} dt
\end{aligned} \tag{10}$$

where we used the property of the triple product to simplify the expression $\vec{A} \cdot (\vec{B} \times \vec{C}) = \vec{B} \cdot (\vec{C} \times \vec{A}) = \vec{C} \cdot (\vec{A} \times \vec{B})$.

The integrand of the last term in (10) is:

$$\vec{\omega}' \cdot \vec{\tau}' = \vec{\omega} \cdot \vec{\tau} = I\omega_1\dot{\omega}_1 - \cancel{(I - I_3)\omega_1\omega_2\omega_3} + I\omega_2\dot{\omega}_2 - \cancel{(I_3 - I)\omega_2\omega_3\omega_1} + I_3\omega_3\dot{\omega}_3 \tag{11}$$

where the covariance of scalar products under rotations was used to transition from the fixed orientation system (S') to the body system (S), and then the torque components were substituted using the Euler equations for the motion of rigid bodies [5]. Thus, we have that the integral in the last term is:

$$\begin{aligned}
\int_0^{\Delta t_1} \vec{F}_{\text{contact}} \cdot (\vec{\omega}' \times \vec{r}) dt &= \int_0^{\Delta t_1} \vec{\omega}' \cdot (\vec{r} \times \vec{F}_{\text{contact}}) dt \\
&= \int_0^{\Delta t_1} \vec{\omega}' \cdot \vec{\tau}' dt = \int_0^{\Delta t_1} (I\omega_1\dot{\omega}_1 + I\omega_2\dot{\omega}_2 + I_3\omega_3\dot{\omega}_3) dt \\
&= \frac{I\omega_{1,1}^2}{2} + \frac{I\omega_{2,1}^2}{2} + \frac{I_3\omega_{3,1}^2}{2} - \frac{I\omega_{1,0}^2}{2} - \frac{I\omega_{2,0}^2}{2} - \frac{I_3\omega_{3,0}^2}{2}
\end{aligned} \tag{12}$$

The integral in the penultimate term of (10) is:

$$\int_0^{\Delta t_1} \vec{F}_{\text{contact}} \cdot \vec{V} dt = \int_0^{\Delta t_1} \vec{F} \cdot \vec{V} dt + \int_0^{\Delta t_1} \vec{f} \cdot \vec{V} dt \tag{13}$$

where \vec{F} and \vec{f} can be determined using the second Newton's law:

$$\frac{d\vec{p}}{dt} = \vec{F} + \vec{f} + M\vec{g} \Rightarrow M \frac{d}{dt} \left\{ V_\rho \hat{\rho} + V_n \hat{n} + V_3 \hat{e}'_3 \right\} = f_\rho \hat{\rho} + f_n \hat{n} + (F - Mg) \hat{e}'_3$$

and noting that $\frac{d\hat{\rho}}{dt} = \omega'_3 \hat{e}'_3 \times \hat{\rho} = \dot{\phi} \hat{n}$ and $\frac{d\hat{n}}{dt} = \omega'_3 \hat{e}'_3 \times \hat{n} = -\dot{\phi} \hat{\rho}$, we get:

$$F = Mg + M \frac{dV_3}{dt}, \quad f_\rho = -M\dot{\phi}V_n + M \frac{dV_\rho}{dt}, \quad f_n = M\dot{\phi}V_\rho + M \frac{dV_n}{dt} \tag{14}$$

Thus, the integrals in (13) become:

$$\int_0^{\Delta t_1} \vec{F} \cdot \vec{V} dt = \int_0^{\Delta t_1} \left(Mg + M \frac{dV_3}{dt} \right) V_3 dt = \left(\frac{MV_{3,1}^2}{2} + Mgh_1 \right) - \left(\frac{MV_{3,0}^2}{2} + Mgh_0 \right) \quad (15)$$

which affects the height of the cylinder and the vertical component of the CM velocity after the collision, and

$$\begin{aligned} \int_0^{\Delta t_1} \vec{f} \cdot \vec{V} dt &= \int_0^{\Delta t_1} (f_\rho \hat{\rho} + f_n \hat{n}) \cdot (V_\rho \hat{\rho} + V_n \hat{n} + V_3 \hat{e}'_3) dt = \int_0^{\Delta t_1} (f_\rho V_\rho + f_n V_n) dt \\ &= \int_0^{\Delta t_1} \left(MV_\rho \frac{dV_\rho}{dt} - \cancel{M\dot{\phi}V_\rho V_n} + MV_n \frac{dV_n}{dt} + \cancel{M\dot{\phi}V_n V_\rho} \right) dt = \frac{MV_{h,1}^2}{2} - \frac{MV_{h,0}^2}{2} \end{aligned} \quad (16)$$

where $V_h = \sqrt{V_\rho^2 + V_n^2}$ represents the horizontal component of the CM velocity. The component of \vec{V} along \hat{e}'_3 , V_3 , does not contribute to the calculation of the term in expression (16).

Assuming that the cylinder rotates around the contact point without sliding for most of the collision time, the components of \vec{V} that form V_h will be given by: $V_\rho = \omega_n h$ and $V_n = -(\omega_\rho h + \omega'_3 \rho)$. It can be observed that $V_\rho \propto \omega_n$, which means that as the cylinder collides and loses angular velocity around the nodal axis (which is what can cause the transition from a “side” to a “face” state and vice versa), it stops moving in the $\hat{\rho}$ direction. On the other hand, V_n consists of two terms, one proportional to ω_ρ and the other proportional to $\omega'_3 = \dot{\phi}$. These angular velocity components can be written as:

$$\begin{aligned} \omega_n &= \vec{\omega}' \cdot \hat{n} = \omega'_1 \cos \phi + \omega'_2 \sin \phi \\ \omega_\rho &= \vec{\omega}' \cdot \hat{\rho} = -\omega'_1 \sin \phi + \omega'_2 \cos \phi \end{aligned} \quad (17)$$

which is a system that can be solved for ω'_1 and ω'_2 , yielding:

$$\begin{aligned} \omega'_1 &= -\omega_\rho \sin \phi + \omega_n \cos \phi \\ \omega'_2 &= \omega_\rho \cos \phi + \omega_n \sin \phi \end{aligned} \quad (18)$$

so that when the die is no longer toppling ($\omega_n \rightarrow 0$), the die will still be rolling with $\omega_3 = \omega_\rho$.

Substituting the results (12), (15), and (16) into (13), we have:

$$\begin{aligned}
W_1 = & \frac{MV_{3,1}^2}{2} + \frac{MV_{h,1}^2}{2} + Mgh_1 - \frac{MV_{3,1}^2}{2} - \frac{MV_{h,0}^2}{2} - Mgh_0 \\
& + \frac{I\omega_{1,1}^2}{2} + \frac{I\omega_{2,1}^2}{2} + \frac{I_3\omega_{3,1}^2}{2} - \frac{I\omega_{1,0}^2}{2} - \frac{I\omega_{2,0}^2}{2} - \frac{I_3\omega_{3,0}^2}{2}
\end{aligned} \tag{19}$$

After the first collision, the energy will be $E_1 = E_0 + W_1$, and after successive collisions, we have:

$$E_n = E_0 + W_1 + W_2 + \dots + W_n = K + Mgh_n \tag{20}$$

where the various dissipative terms cancel out terms from previous terms and convert kinetic energy into other forms of energy. In the end, only the potential energy associated with the height of the CM remains, plus an additional term K that will be zero for the “face” states and equivalent to a kinetic energy $\frac{1}{2}(MV^2 + I_3\omega_3^2)$ for the “side” state.

C. The statistics of the results of cylinder tosses

It is obvious, at this point, that it would be a terrible idea to try to analyze the motion, even of a single die, from a deterministic perspective. Small perturbations in the initial conditions and the characteristics of the point of contact with the surface of the landing plane would already result in significant differences in the sequence of movements. The explanations in the previous sections, therefore, do not intend to follow that path but rather to glimpse the characteristics of the motion, infer qualitatively what to expect from it, and finally, understand how the definition of a “face” or “side” state will be associated with a certain amount of energy that remains after a toss and the subsequent collisions that follow.

Hence, given the dimensions of a given cylinder, it can end up in a “side” state with energies $E_S(V)$ or “face” state with energy E_F . Thus, a die is a two-level system.

If dice are placed on a plane that ejects them, constantly shaking and causing a sequence of random collisions, we can say that these dice receive an average energy from this plane, which is partly converted into potential energy, propelling the dice upward, partly into translational kinetic energy, and partly into rotational kinetic energy. Thus, the dice have a certain probability of receiving energy from the landing/launching plane and then retaining part of that energy according to the discussion in the previous section. If we think of a large number of identical copies of this system that launch dice and where dice have a certain

probability of receiving energy, the comparison with a canonical ensemble where multiple systems are in contact with a certain thermal reservoir at temperature T is inevitable. A canonical ensemble, in turn, follows a Boltzmann probability distribution function [6].

It is evident, however, that this idea, although aesthetically appealing, is limited, especially because it would be impractical to launch a large number of cylindrical dice on the order of 1 mol. Nevertheless, we will work with this hypothesis.

1. Statistics of free fall

We can start by revisiting Equation 2, which describes the energy of a cylinder during free fall. Knowing this, we can calculate the partition function and, subsequently, the average energy of this system as a function of $\beta = 1/(k_b T)$. For this purpose, we define Z_{pot} , Z_{kin} , and Z_{rot} , which, when multiplied, result in the desired partition function Z .

$$\begin{aligned} Z_{pot} &= \int_0^{\infty} e^{-\beta Mgh} dh \\ Z_{kin} &= \left(\int_{-\infty}^{\infty} e^{-\beta \frac{MV^2}{2}} dV \right)^3 \\ Z_{rot} &= \left(\int_{-\infty}^{\infty} e^{-\beta \frac{I\omega^2}{2}} d\omega \right)^2 \int_{-\infty}^{\infty} e^{-\beta \frac{I_3\omega_3^2}{2}} d\omega_3 \end{aligned} \quad (21)$$

The value of Z_{pot} introduces the gravitational potential energy. The values of Z_{kin} and Z_{rot} introduce, each, 3 degrees of freedom related to translational and rotational kinetic energies, respectively. After performing the integrals, we can calculate Z :

$$Z = \frac{8\pi^3}{I\sqrt{I_3}\beta^4 g M^{\frac{5}{2}}} \quad (22)$$

The average energy is given by:

$$\langle E \rangle = -\frac{1}{Z} \frac{dZ}{d\beta} = \frac{4}{\beta} \quad (23)$$

By isolating β , it is possible to find this value as a function of the average energy of the system. However, this energy depends on time since there is dissipation due to collisions. Thus, we have:

$$\beta(t) = \frac{4}{\langle E(t) \rangle} \quad (24)$$

Note that in Z_{pot} , the height h was integrated with a lower limit of 0. This means that the reference for gravitational potential energy was shifted from the ground to the minimum height, making the involved calculations simpler. Therefore, this energy present in the β formula is actually an energy variation, i.e., the energy received by the plane minus the dissipated energy in collisions.

2. Statistics of the final state

Having done that, it is necessary to consider the final state. Unlike free fall, the cylinder is forced to assume one of the two previously mentioned states: “face” or “side”. Knowing the energies of each state, we can write a new Boltzmann distribution, with different partition function and probabilities from the previous section.

The energy of the “side” state is given by:

$$E_S = Mgh_S + K = MgR + \frac{3MV^2}{4} \quad (25)$$

where the value of kinetic energy K was calculated considering a rolling without slipping constraint. However, the kinetic energy must be understood as a second possibility, meaning that the cylinder can fall into this state with only potential energy or with the presence of kinetic energy.

The energy of the “face” state is:

$$E_F = Mgh_F = \frac{MgH}{2} \quad (26)$$

Thus, we can calculate the respective probabilities. Let P_S be the probability of observing the die in the “side” state, and $q = H/R$:

$$P_S = \frac{1}{Z} \left(\frac{1}{Z'} C_S \int_0^\infty 2\pi V e^{-\beta(MgR + \frac{3MV^2}{4})} dV + C_S e^{-\beta MgR} \right) \quad (27)$$

where C_S is a coefficient related to the multiple ways of finding the “side” state with the same energy, and Z' is a proportionality constant, which will be both discussed later.

Since a velocity vector of magnitude V can point in different directions in space, we also needed to consider these possibilities, and for that, we think in terms of velocity space. An area element dA in this space can be calculated as:

$$dA = \int_0^{2\pi} d\theta \int_V^{V+dV} r dr = 2\pi V dV \quad (28)$$

thus, the term $2\pi V$ present in the expression was explained.

However, upon analyzing the dimension of the term resulting from the integral, it is noticed that it has units of velocity squared. As a probability must be dimensionless, we added the element $1/Z'$, with Z' having the same unit as the term in question, so the dimensions cancel out.

Traditionally, velocity space would be used for comparisons between restricted areas or volumes and the total. A clear example is the calculation of the probability of finding a particle in a gas within a certain range of velocity magnitudes, by comparing a specific volume, represented by a sphere, with respect to the total volume of space. It is evident that neither the total volume nor the partial volume represents the actual number of microstates, but they are proportional to these values, enabling the calculation of probabilities.

In the discussed case, we have to compare a term calculated using velocity space with another in which this was not used, which is, at first, incompatible. However, we know that the quantity of microstates is proportional to the result of the integral, so the sought-after value must be this result multiplied by a constant $1/Z'$. Although we do not know the value of Z' , we can speculate that it represents an area in velocity space:

$$Z' = \pi V_{Z'}^2 \quad (29)$$

in which $V_{Z'}$ can be something like the typical or the maximum velocity reached by the cylinders.

The expression for the probability of the “face” state is considerably simpler, due to the absence of kinetic energy:

$$P_F = \frac{1}{Z} C_F e^{-\beta E_F} \quad (30)$$

and here, once again, C_F is a coefficient related to the multiple ways of finding the “face” state with the same energy.

Having done that, we are in a position to solve the integral of P_S , calculate the partition function by normalization, and write the probabilities. However, the coefficients of multiplicity to be calculated still remain. Hence, the expression for P_S becomes:

$$P_S = \frac{C_S e^{-\beta M g R} + \frac{1}{Z'} \frac{4\pi}{3\beta M} C_S e^{-\beta M g R}}{C_F e^{-\beta \frac{M g R q}{2}} + C_S e^{-\beta M g R} + \frac{1}{Z'} \frac{4\pi}{3\beta M} C_S e^{-\beta M g R}} \quad (31)$$

3. Calculation of C_S and C_F

Before we proceed with the calculation itself, let's elaborate a bit more on the need for these coefficients. Imagine that, instead of cylinders, the solids in question were pyramids. Intuitively, we know that it is impossible for such a pyramid to come to rest balanced on its vertex without piercing the surface or being glued to it. This is due to the lack of stability of this state, which would quickly transform into a state balanced on one of the faces of the pyramid. However, if we were to write the probability of this state, it would be extremely higher than what is observed experimentally because the multiple ways of finding each state with the same energy were not taken into account. To overcome this problem, we introduce these coefficients.

For the calculation of these values, we will consider a sphere circumscribed around the cylinder (see Figure 3). Imagine a cylinder in free fall, but in the reference frame of the object itself. In this case, the ground would be approaching, and all the different ways that could happen would form a sphere around the cylinder. Certain parts of the sphere are associated with a collision on the face part, A_F , and others on the side part, A_S . Thus, we will propose that the area corresponding to each part, divided by the total area of the sphere, is equivalent to the coefficient of the respective state.

$$A_F = 2 \int_0^{2\pi} d\phi \int_0^{\theta_L} R^2 \sin \theta d\theta \quad (32)$$

$$A_S = 4\pi R^2 - A_F \quad (33)$$

Thus, we can write the coefficients:

$$C_S = \frac{A_L}{4\pi R^2} = \left(\frac{q}{\sqrt{q^2 + 4}} \right) \quad (34)$$

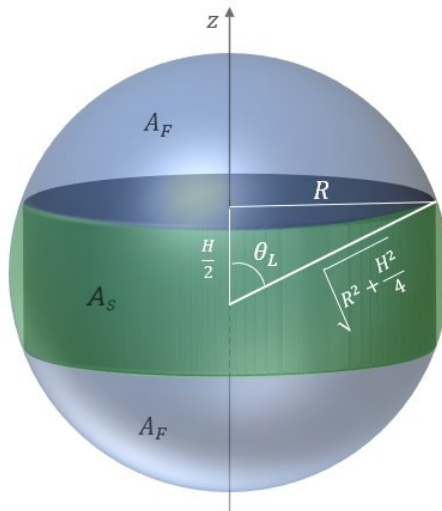


FIG. 3: Sphere circumscribed around the cylinder.

$$C_F = \frac{A_F}{4\pi R^2} = \left(1 - \frac{q}{\sqrt{q^2 + 4}}\right) \quad (35)$$

Note that these values are normalized, i.e., they range from 0 to 1 and sum up to 1. Mathematically, $C_F + C_S = 1$.

4. Estimating β

According to Equation 24, the final value of β occurs when $t \rightarrow \infty$. To calculate this value, we need to know the final average energy, which can be written as follows:

$$\langle E_f \rangle = \langle E_0 \rangle + \langle W \rangle \quad (36)$$

where $\langle E_0 \rangle$ is the average energy received from the plane and $\langle W \rangle$ is the sum of the energies dissipated after successive collisions.

In order to estimate the value of $\langle W \rangle$, we will propose that there are two types of collisions. The first type is related to a collision in the A_F region, while the second type is related to a collision in the A_S region. Thus, we will also assume the existence of two types of work, related to a series of collisions in each of these areas. If $\langle W \rangle = W_F$, only collisions in A_F have occurred. On the other hand, if $\langle W \rangle = W_S$, only collisions in A_S have occurred.

It is clear that these two cases are unreal, and a combination of these two types of collisions is expected. The coefficients of multiplicity, calculated earlier, can indicate the contribution expected from each type of work. For example, if $C_S = 0.7$ and $C_F = 0.3$, it is expected that 7 out of 10 collisions have occurred in the A_S region. Similarly, we can use the same relationships for the works:

$$\langle W \rangle = C_F W_F + C_S W_S \quad (37)$$

However, it is obvious that this proposal is only an approximation. It is evident that there is variation in the values of W_S and W_F even if the collisions are in their respective regions, i.e., depending on how this collision occurs, there will be more or less dissipation. This estimation method will be more efficient in cases where a higher collision rate is not forced in any of the regions, which is valid for the experiment of the plane ejecting cylinders. However, if the cylinders are horizontally launched and always in the same way, there will be a greater tendency for collision in a specific manner, causing the coefficients to have values that diverge from what is observed, requiring a correction.

Furthermore, it is important to note that the absolute value of W_F should be greater than the absolute value of W_S . This occurs because the “side” state allows for rolling, dissipating less energy as it remains in the form of rotation.

III. EXPERIMENTAL DESCRIPTION

A. Used Equipment and Experimental Setup

As described in the theoretical fundamentals section, the launch conditions of the cylinder greatly affect P_S and P_F . Therefore, it is necessary to develop an experiment to standardize each repetition. Considering the need for a large data sample, the solution found was the construction of a machine using Arduino and, subsequently, a program in the Python programming language to recognize the two possible states, “face” and “side”, and calculate their respective probabilities.

A box made of medium-density fiberboard (MDF) was used to house the entire experiment. The base, with a thickness of 6 mm, has a cavity with a depth of 3 mm, where the protoboard (a board used for circuit assembly) was inserted. The side walls of the box were

made of the same material as the base and half the thickness, i.e., 3 mm. Structures for support and connection between the walls were 3D printed using polylactic acid (PLA). Two cardboard sheets, one covered with sulfite paper and the other with suede, were also prepared as surfaces for launching the cylinders.

The cylinders used were 3D printed in white PLA with a 25% infill, and each face of the same cylinder was painted blue and red, respectively, for recognition purposes. The radius was kept constant at 7.5 mm, and the H/R ratios varied from 0.3 to 2.5 with intervals of 0.1.



FIG. 4: Cylinders used in the experiments.

For the assembly of the electrical system (Figure 5), an Arduino UNO board was used, as well as 8 JF-0530B model solenoids, each with a force of 5 N, controlled by relays (electromechanical switches). To provide the necessary voltage for the motor operation, a regulated DC power supply with a voltage of 22 volts was used. For image capture, a Logitech C920 camera positioned above the box, fixed on a universal stand, was controlled by a computer program.

With all the mentioned components, the system was assembled (Figure 6), with the solenoids reaching the cardboard plate, lifting it and performing a launch.

Additionally, for the determination of some parameters, namely the coefficient of restitution (ε), the average height reached by the cylinders (\bar{h}), and the static and kinetic friction coefficients (μ_s and μ_k), the system was modified. For the first two parameters, the system was set up without the front wall, and the camera was repositioned to capture the movement from the front (Figure 8(a)). For the friction coefficients, the sulfite-coated cardboard plate

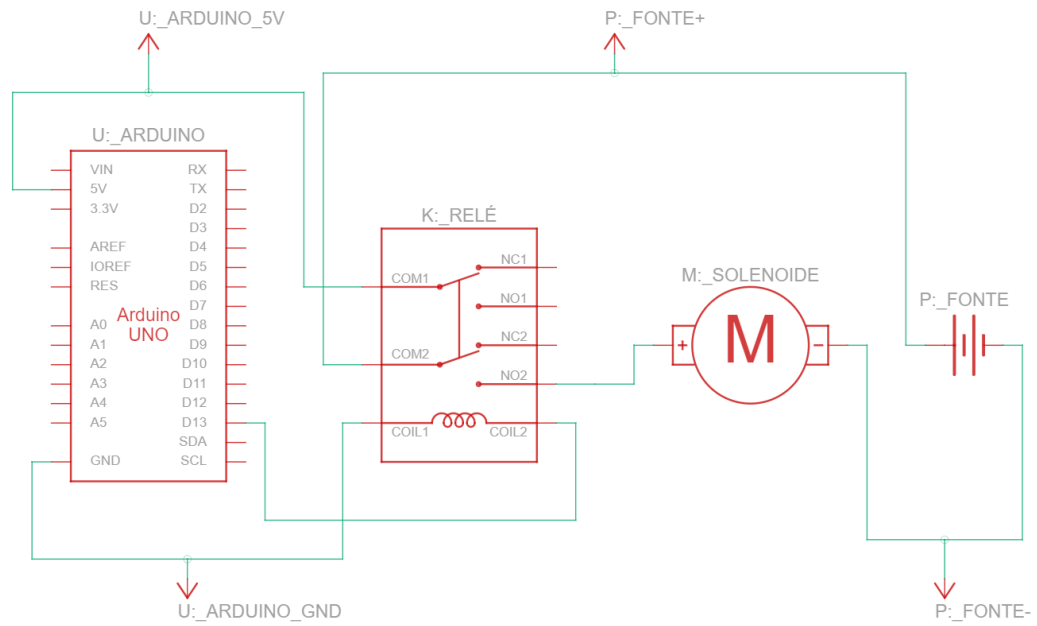


FIG. 5: Electrical schematic of the system for a single solenoid.

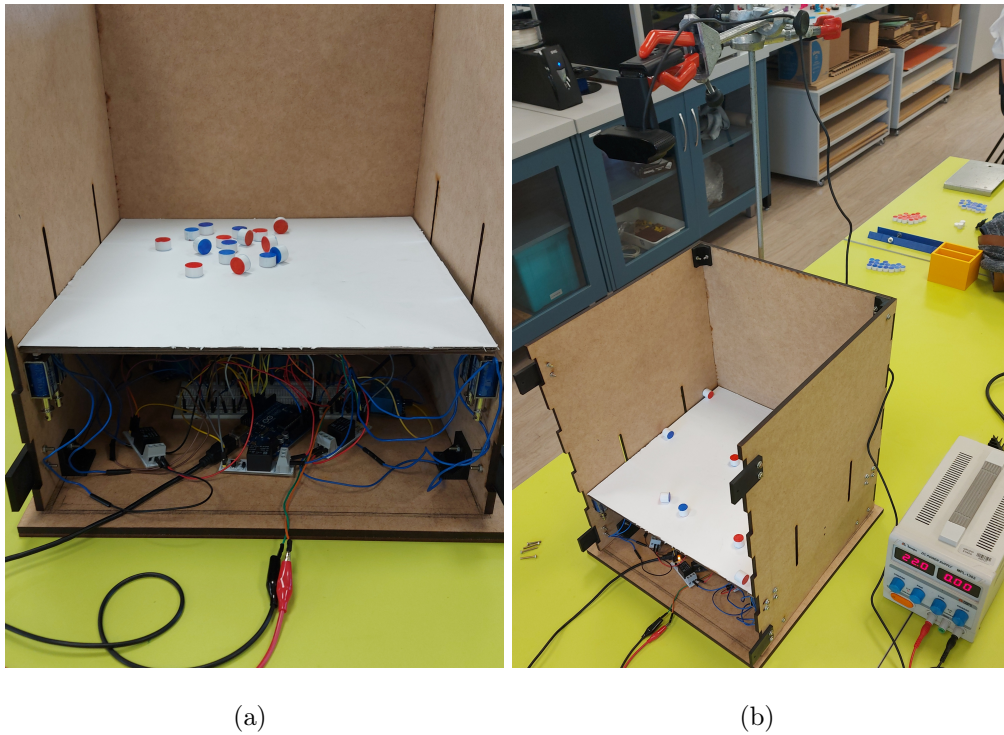


FIG. 6: (a) Front view of the system; (b) Complete view of the system with the camera.

was placed on an inclined plane, and the sliding of a cylinder was analyzed.

B. Procedure

With the system assembled, a Python program was executed to control the Arduino and, consequently, the movement of the solenoids through serial signals. The solenoids hit the cardboard plate on which the cylinders were placed, launching them. After the launch, the program waited for 5 seconds to allow the cylinders to stabilize and then activated the camera to capture an image (Figure 7(a)) of the cylinders in their respective final states (“face” or “side”).

This process was repeated two hundred times for each H/R ratio (ranging from 0.3 to 2.5).

Through this procedure, it was possible to automatically obtain hundreds of photos per hour, thus obtaining a large sample. To analyze the final state of each cylinder, a second algorithm was programmed to recognize circles and colors (Figure 7(b)) and identify whether they were in the “face” or “side” state.

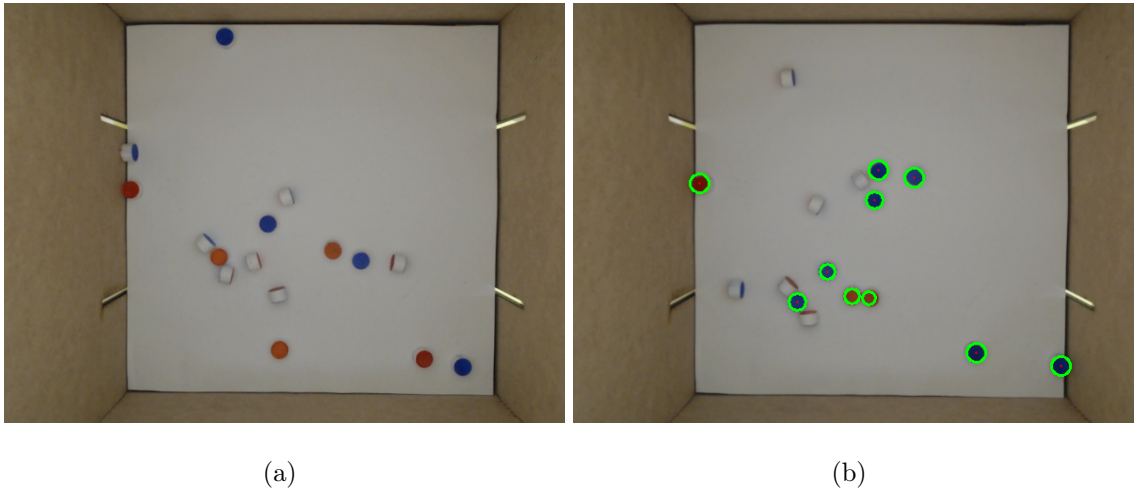


FIG. 7: (a) Image captured by the camera; (b) Circle recognition by the algorithm.

Knowing the number of times the final result was “face” or “side” and the total number of launches, the probability of each state was calculated, and experimental graphs of P_L and P_F as a function of the H/R ratio (which can also be expressed solely as a function of H since R was kept constant) were created using these data points.

By modifying the system for the setup with the front-facing camera (Figure 8(a)), the average height (\bar{h}) and the coefficient of restitution (ε) were determined. A millimeter grid

paper was used on the back wall of the box (Figure 8(b)) to enable measurement.

Simultaneously, experiments were conducted to determine the friction coefficients. For the static coefficient, the plate was placed on the plane without inclination, and the angle was gradually increased until the sliding threshold was reached. For the kinetic coefficient, the plate was inclined above the maximum angle of static friction, and a cylinder was released, with the time of motion measured.

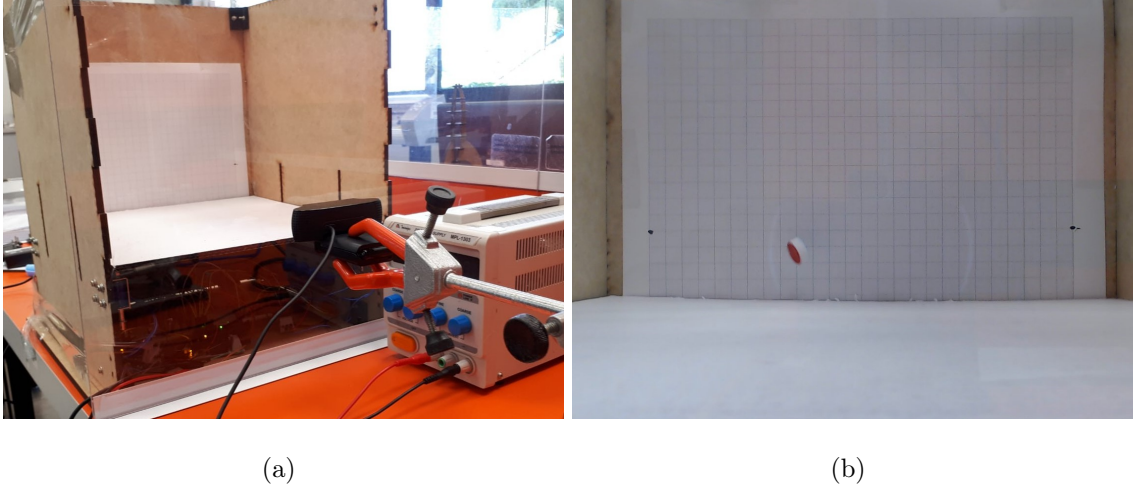


FIG. 8: (a) Image of the system with the front-facing camera positioned; (b) Image captured by the camera with the position of the grid paper.

C. Secondary Experiment: Horizontal Launch

Although the developed theory is much more adapted to the machine case, we also created a second experiment to test the limits of this formulation. For a horizontal launch, there is a significant increase in velocity in that direction, inducing collisions in a specific region. This situation falls into what was discussed in the estimation of β (Section II C 4) and requires a correction in the multiplicity coefficients.

For this experimental setup, equipment similar to a catapult was used, which operates based on a counterweight. In this way, it is possible to ensure the same initial energy for all cylinders, which will be horizontally launched.



FIG. 9: Image of the experimental setup for horizontal launch.

IV. DISCUSSION AND DATA ANALYSIS

A. Obtained Results

To analyze the probabilities of each state for each H/R ratio, the first step was to determine \bar{h} . The experimentally obtained result was: $\bar{h} = 3.8$ cm for $q = 1$. With this value, it is possible to calculate the energy supplied by the plane to the cylinders.

The second step would be to calculate the values of W_S and W_F . However, the calculation of these numbers, both theoretically and experimentally, remains as a topic for future research. Thus, an adjustment was made for these values, and for better understanding, they were normalized by dividing them by E_0 . To perform the adjustment, the computer program starts with both values set to 0.5 and adjusts them in small increments until the standard deviation of the theoretical and experimental values is minimized.

Starting with the results obtained with sulfite paper, the fit resulted in the values given in (38).

$$\begin{aligned} W_S &= 0.475 \pm 0.001 \\ W_F &= 0.999 \pm 0.001 \end{aligned} \tag{38}$$

from which we have graphs of W and β as functions of q .

Moving on to the results obtained with suede fabric, the fit resulted in the values given in (39).

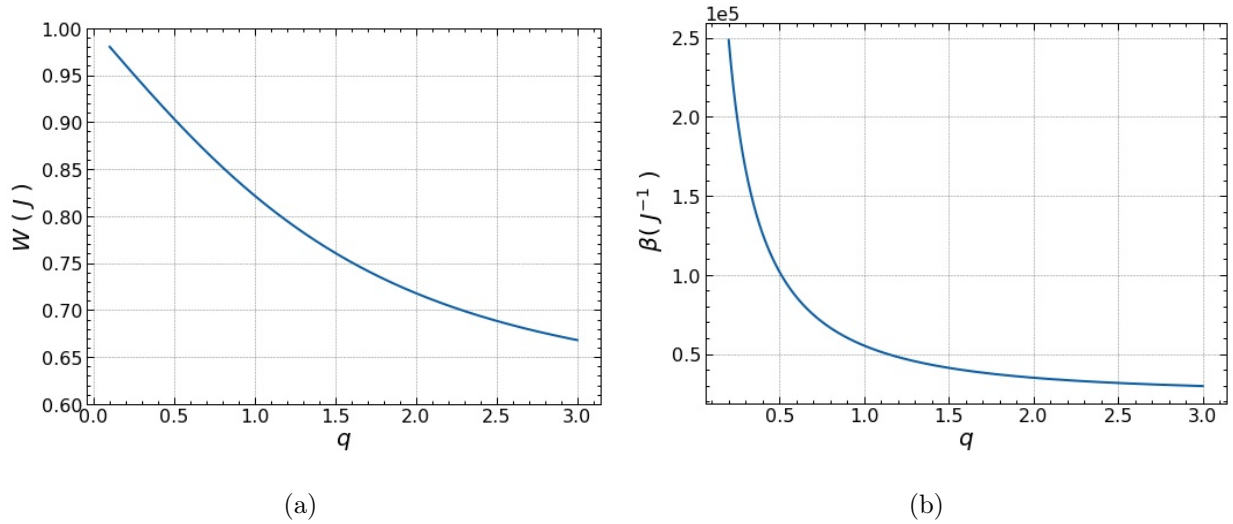


FIG. 10: Graphics for sulfite paper in the machine displaying (a) W , and (b) β as functions of q .

$$\begin{aligned}
 W_S &= 0.836 \pm 0.001 \\
 W_F &= 0.878 \pm 0.002
 \end{aligned}
 \tag{39}$$

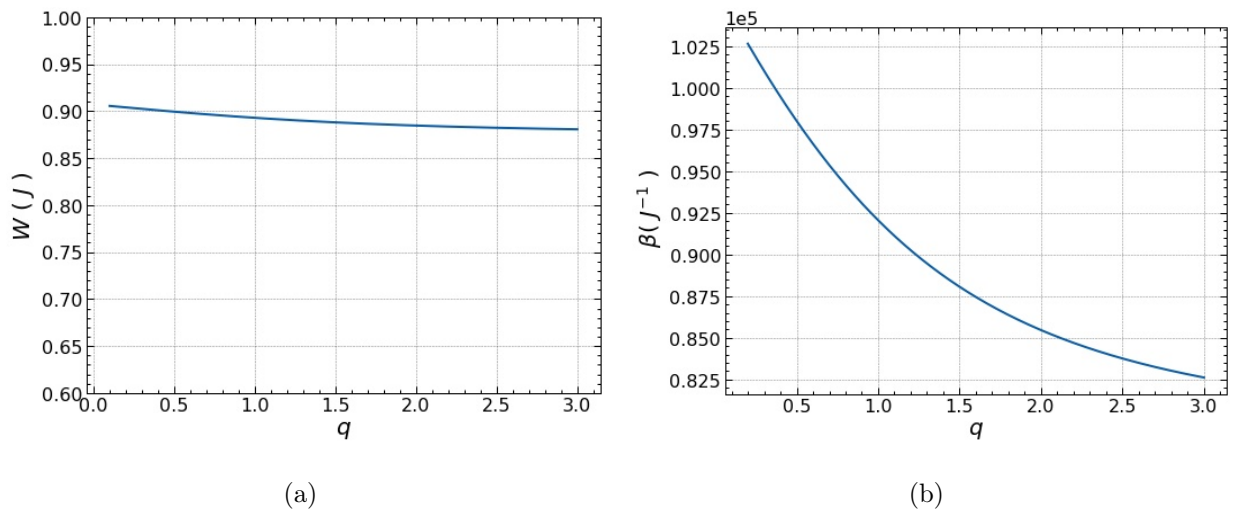


FIG. 11: Graphics for suede fabric in the machine displaying (a) W , and (b) β as functions of q .

Finally, in Figure 12, we have the graphs of P_S as a function of q being compared with the experimental results obtained.

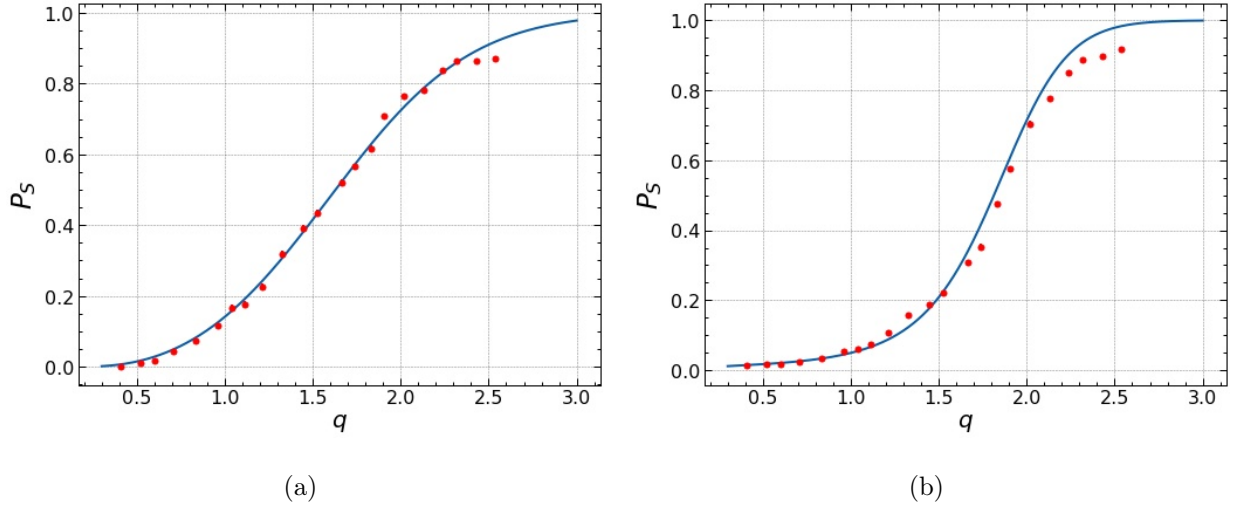


FIG. 12: Graphics of P_S as a function of q in the machine for (a) sulfite paper, and (b) suede fabric.

B. Horizontal Launch

With the help of the Tracker software, we can calculate the velocity and height at which the cylinders are ejected and, therefore, the energy supplied. The fits for the values of W_S and W_F are as follows for each surface.

For sulfite paper, we found the values given in (40).

$$\begin{aligned} W_S &= 0.00 \pm 0.01 \\ W_F &= 1.142 \pm 0.001 \end{aligned} \tag{40}$$

and, as we did before for the machine, we produced the resulting graphs for these values, which can be seen in Figure 13.

For suede fabric, the values found were those given in (41).

$$\begin{aligned} W_S &= 0.000 \pm 0.005 \\ W_F &= 1.3118 \pm 0.0005 \end{aligned} \tag{41}$$

with resulting graphs shown in Figure 14.

The respective results for P_S as a function of q can be seen in Figure 15.

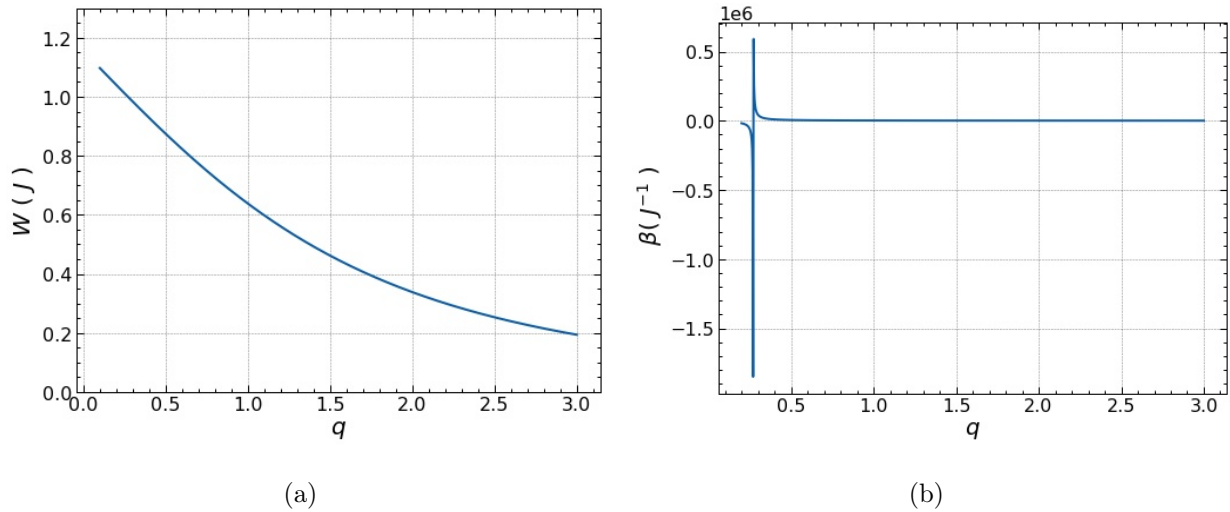


FIG. 13: Graphics for sulfite paper in the horizontal launch displaying (a) W , and (b) β as functions of q .

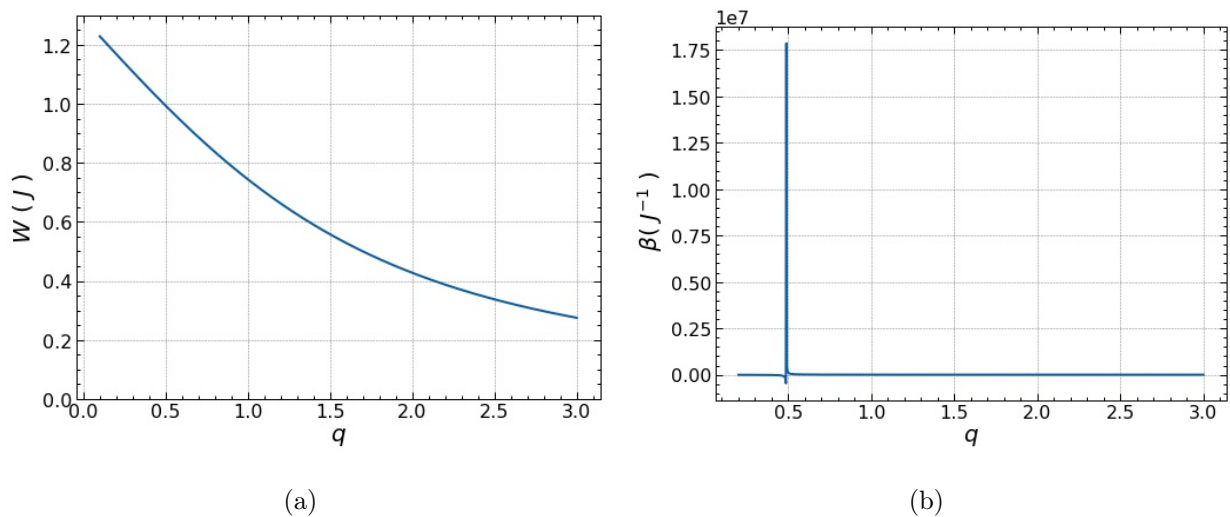


FIG. 14: Graphics for suede fabric in the horizontal launch displaying (a) W , and (b) β as functions of q .

C. Discussion of Results

Analyzing the results of the experimentally obtained probabilities and adjusting the theoretical curves, it can be observed that the data, in general, behave as expected for the machine. However, there are deviations, as expected, considering that 200 launches were

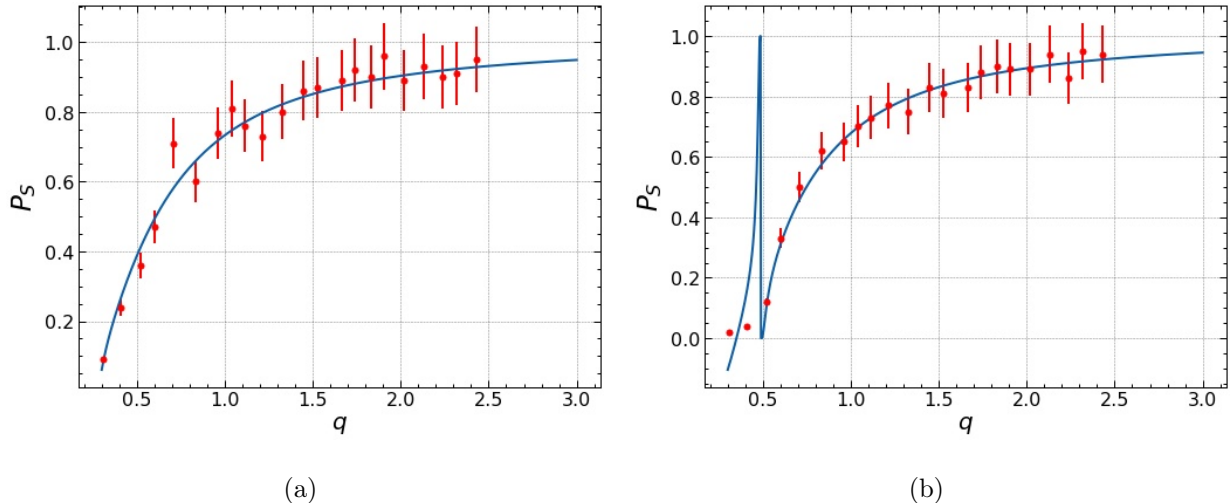


FIG. 15: Graphics of P_S as a function of q in the horizontal launch for (a) sulfite paper, and (b) suede fabric.

performed for each H/R ratio, with 16 cylinders in each launch, resulting in a total of 3200 cylinders launched for each ratio, which is still a small number compared to 1 mol.

These deviations are mainly due to experimental errors, limitations, and theoretical approximations. Possible sources of experimental errors include problems with computational recognition or, perhaps, wear and deformation of materials due to repeated use. Additionally, the experiment with the suede material was conducted after the one with the sulfite paper, which means that the materials were much more worn, and it is precisely in this experiment that the largest divergences from the expected results occurred. As for the limitations in theory, they are due to certain factors that were not considered in the calculation of E and, of course, the fact that the number of data points is small compared to the statistical limit ($N \sim 1$ mol).

Thus, by analyzing the behavior of the experimental data and the adjusted curve, it is possible to determine the ideal H/R ratio for specific conditions, such as materials and launching methods.

For the secondary experiment, the discrepancies are significant for two main reasons. Firstly, only 200 launches were performed for each ratio, which is a much smaller number of repetitions compared to the machine experiment and further away from 1 mol. Secondly, this launching method favors certain forms of collision, which means that the calculated

multiplicity coefficients are not appropriate. This is reflected in the fact that the values of W_F are greater than 1, which should not occur since the dissipation cannot be greater than the initial energy. However, this unexpected value exists to compensate for a very low value of C_F . Despite these anomalies, which generate peaks in the graphs, the probabilities reasonably correspond to what was theoretically predicted for larger ratios.

V. CONCLUSIONS

Therefore, it can be concluded that the developed theory provides a reasonable approximation for the probabilities of final states of a cylinder based on its H/R ratio, through experimental adjustments. However, it would be possible to obtain the theoretical values of the factors used in the adjusted function by improving the experimental conditions and extending the data analysis to consider other aspects. This would enable a comparison between the adjusted values and the corresponding theoretical curve.

Furthermore, it remains to explore more thoroughly various possible variations of the system, such as different surfaces (beyond the two already used), thus modifying the coefficients of friction and restitution, which should be taken into account in a more detailed future analysis. These factors can likely be considered after further development of the theory. Additionally, limitations of the theoretical approach through Statistical Mechanics persist.

The horizontal launch clearly demonstrates the limitations of what has been developed so far. In future analyses, as a way to complement what has already been done, a more detailed calculation of the multiplicity coefficients and the work done in collisions is needed.

Despite its limitations, the theory discussed has applications that go beyond a specific solid. For example, if a solid has a symmetry such that the energy of each state is the same and the multiplicity coefficients are also the same, it is possible to affirm that this solid is a “fair die” regardless of the initial energy and the launching method. In other words, it presents the same probabilities of falling for all faces (provided that collisions are not induced in a specific region, altering the multiplicity factors). An example of this is RPG dice, which are Platonic solids and exhibit this symmetry, including, of course, the case of the traditional six-sided die.

Last but not least, it is worth to mention that this investigation was completed as part

of the authors' participation in the International Young Physicists' Tournament (IYPT), a competition that seeks to encourage high school students to solve open physics problems which consist of small paragraphs defining a specific situation or phenomenon, and then establish some task that will not have a final or closed answer but will lead students to find creative and deep explanations for that situation. Ordinary high school physics will certainly not be enough to accomplish those tasks and, therefore, those students will learn much more than what is usually taught in regular curricula. These are, therefore, typical characteristics of an active learning method.

Acknowledgments

We would like to thank Prof. Silvio R. A. Salinas from the University of São Paulo for his supportive opinions and discussion on the statistical mechanics of the three-sided dice.

-
- [1] IYPT. International Young Physicists' Tournament. <<https://www.iypt.org>>.
 - [2] IYPT. International Young Physicists' Tournament 2022 Problems. <<https://www.iypt.org/problems/problems-for-the-35th-iypt-2022/>>.
 - [3] P. Diaconis and J. B. Keller. *Am. Math. Mon.*, Vol. 96, No. 4. (Apr., 1989), pp. 337-339.
 - [4] J. B. Keller. *Am. Math. Mon.*, Vol. 93, No. 3. (Mar., 1986), pp. 191-197.
 - [5] Thornton & Marion, *Classical Dynamics of Particles and Systems*. Brooks/Cole - Thomson Learning, 2004 (5th ed).
 - [6] S. J. Blundell & K. M. Blundell, *Concepts in Thermal Physics*. Oxford University Press, 2010 (2nd ed).
 - [7] S. R. A. Salinas, *Introduction to Statistical Physics*. Springer, 2001.
 - [8] R. Cross, *Sports Technology*, **3:3**, (2010) 168-180. DOI: 10.1080/19346182.2011.564283